Digital Discovery

ROYAL SOCIETY OF CHEMISTRY

PAPER

View Article Online
View Journal | View Issue

Cite this: *Digital Discovery*, 2023, **2**, 799

Automated electrolyte formulation and coin cell assembly for high-throughput lithium-ion battery research

Jackie T. Yik, *[a] Leiting Zhang, *[a] Jens Sjölund, [b] Xu Hou,[a] Per H. Svensson, [cd] Kristina Edström[a] and Erik J. Berg [a]

Battery cell assembly and testing in conventional battery research is acknowledged to be heavily time-consuming and often suffers from large cell-to-cell variations. Manual battery cell assembly and electrolyte formulations are prone to introducing errors which confound optimization strategies and upscaling. Herein we present ODACell, an automated electrolyte formulation and battery assembly setup, capable of preparing large batches of coin cells. We demonstrate the feasibility of Li-ion cell assembly in an ambient atmosphere by preparing $LiFePO_4||Li_4Ti_5O_{12}$-based full cells with dimethyl sulfoxide-based model electrolyte. Furthermore, the influence of water is investigated to account for the hygroscopic nature of the non-aqueous electrolyte when exposed to ambient atmosphere. The reproducibility tests demonstrate a conservative fail rate of 5%, while the relative standard deviation of the discharge capacity after 10 cycles was 2% for the studied system. The groups with 2 vol% and 4 vol% of added water in the electrolyte showed overlapping performance trends, highlighting the nontrivial relationship between water contaminants in the electrolytes and the cycling performance. Thus, reproducible data are essential to ascertain whether or not there are minor differences in the performance for high-throughput electrolyte screenings. ODACell is broadly applicable to coin cell assembly with liquid electrolytes and therefore presents an essential step towards accelerating research and development of such systems.

Received 4th April 2023
Accepted 28th April 2023

DOI: 10.1039/d3dd00058c

rsc.li/digitaldiscovery

Introduction

Global electrification powered by renewable energy sources requires next-generation batteries.[1] However, research and development of new battery chemistries are time-intensive tasks of potentially arduous manual testing that can take decades from initial discovery to commercialization.[1] Therefore, acceleration of research and development is imperative to meet growing demands. Considerable efforts have been made on developing and integrating accelerators (*e.g.* automation, parallelization, data repositories, machine learning models, *etc.*).[2] Although accelerators used in synthesis and characterization of battery materials are becoming mature,[2,3] automation of systems-level applications involving battery assembly and performance testing still have room to improve. Of the few published robotic setups bridging characterization- and systems-level application of the battery materials research workflow, Dave *et al.* reported a robotic setup, called Clio, for the material discovery process of electrolyte formulations that have automated the characterization of electrolyte formulations[4,5] and Zhang *et al.* developed a setup, AutoBASS, automating the battery assembly process with electrolyte dispensing.[6] Matsuda *et al.* also demonstrated a robotic setup, dubbed HTB-system, that has electrolyte formulation and performance testing evaluated in microplates[7] and, more recently, Svensson *et al.* designed a robotic setup, called Poseidon, that has electrolyte formulation and characterization, coin cell assembly and disassembly, and battery evaluation.[8] However, automated batch cell assembly with electrolyte formulation and high rate battery evaluation in a standard cell format has yet to be presented, to our knowledge. We aim to present an alternative robotic setup for the systems-level battery research workflow that has automated electrolyte formulation and dispensing, battery assembly, and electrochemical testing in a standard coin cell format.

A critical part of the battery research process is assembling and performance-testing battery cells. The electrochemical tests alone may take days, months or even years to complete.[9] This manual effort and long testing duration with often limited

[a]*Department of Chemistry, Ångström Laboratory, Uppsala University, P.O. Box 538, SE-751 21 Uppsala, Sweden. E-mail: jackie.yik@kemi.uu.se; leiting.zhang@kemi.uu.se*
[b]*Department of Information Technology, Uppsala University, P.O. Box 337, SE-751 05 Uppsala, Sweden*
[c]*Chemical and Pharmaceutical Development, RISE Research Institutes of Sweden, SE-151 36, Södertälje, Sweden*
[d]*Applied Physical Chemistry, Department of Chemistry, KTH Royal Institute of Technology, SE-114 28, Stockholm, Sweden*

available battery testing channels may partially explain why some battery materials performance studies have data containing only a few replicates. However, human error associated with electrolyte formulations, processing electrodes, and battery assembly give rise to battery performance variations. In order to rely on the results, cell-to-cell variability should be minimized. A study by Dechent *et al.*[10] suggested a minimum of nine replicates to be able to fit a battery aging model with one parameter. The complexity of the system strongly affects the number of replicates required to provide reliable results that can decouple the various effects and reactions in the system.

Moreover, active learning and machine-intelligent decision-making is often coupled with automation to form a "closed-loop" approach to research, where all previously completed steps/experiments inform and decide the following steps, eliminating the archaic "trial-and-error" approaches.[2,11–13] For new battery material discoveries, closed-loop experiments can optimize material selection within a design space quickly, discovering the optimum faster than randomized procedures and with fewer experiments.[14] Within closed-loop approaches, high-throughput screening use automated or semi-automated setups to allow automatic measurements of a defined design subspace at a high rate.[15] The success of high-throughput screening is evident; Yang *et al.*[16] used high-throughput optical measurements to identify regions in three-cation metal oxide composition spaces whose optical trends were not simple phase mixtures, while McCalla *et al.*[17] demonstrated a workflow capable of collecting hundreds of X-ray diffraction patterns and electrochemical impedance spectroscopy spectra, simultaneously, per week.

In this work, we describe an automated robotic setup for electrolyte formulation, assembly and cycling of coin-type battery cells in an ambient laboratory environment. Working in an ambient atmosphere is substantially more cost-effective than maintaining a dry room for cell assembly, potentially opening up the underexplored electrolyte design space with battery materials tolerating ambient atmosphere. Our affordable and easily modifiable setup can be adapted to different systems (*e.g.* non-aqueous electrolytes) with minor alterations; the addition or removal of hardware components can easily be integrated while maintaining, adjusting, or enhancing functionality, characterizing ODACell as a modular setup. The possibility to use ODACell for diverse chemistries generalizes its applicability to explore the high research potential of liquid electrolytes, which have continued to be a challenge to optimize owing to the vast design space.[13] To this end, the objectives of this work are to (1) design and construct an affordable, modular battery assembly and testing setup with electrolyte formulation and dispensing ability, (2) determine the cell-to-cell variability and reproducibility of the system for cells assembled in ambient atmosphere, and (3) demonstrate the setup's practical applicability by preparing and performance-testing hybrid electrolytes containing mixtures of binary solvents, namely water and dimethyl sulfoxide in a full cell configuration.

Methods

Robotic assembly and electrolyte formulation

The robotic setup, ODACell, is shown in Fig. 1A, consisting of three 4-axis robotic arms (Dobot MG400, China) and one liquid handling robot (Opentrons OT-2, USA, Fig. 1B). Each robotic arm was equipped with a unique head for specialized function (Fig. 1C). A custom-made vacuum head holder with two vacuum saving valves (SMC ZP2V, Japan) was set up on one robot allowing it to pick up components; a custom-made claw head and matching holder allowed one robot to collect and move the component stack; and one robot was equipped with an electric gripper (DBT-PGS5, China). A modified electric coin cell crimper (TMAX, China) was connected to interface with the robotic arms, and all robots were fixed to the tabletop. An elevated platform was installed on the tabletop. The platform was used to place custom-made coin cell component trays and holders for battery cycling. Each tray contained enough components for four coin cells and multiple trays were loaded in stacks.

Orchestration of the electrolyte formulation and cell assembly process was done in Python. The full code and data can be found in Github.† Python integration was included with the software development kits of the liquid handling robot and robotic arms. Low-level proprietary functions were wrapped together to form custom, specialized high-level functions for each robot. Commands execute the high-level functions sequentially *via* position triggers to perform specific tasks.

Material selection and preparation

$LiFePO_4$ (lithium iron phosphate, LFP) cathode and $Li_4Ti_5O_{12}$ (lithium titanate, LTO) anode were selected for their known structural and cycling stability[18,19] as well as their commercial availability. Considering the focus of this study was on the robotic setup and reproducibility, commercial electrodes provide highly reliable mass loading, eliminating a potential source of error. A dimethyl sulfoxide (DMSO, $(CH_3)_2SO$)-based electrolyte was selected because of its environmental sustainability[20] and potential for high-voltage applications.[21]

CR2025 coin cell parts (316 stainless steel) were used as received. LFP cathode and LTO anode sheets were ordered from Custom-Cells, Germany. The manufacturer specified specific capacity was 150 mA h g^{-1} for both cathode and anode sheets. Cathode and anode with 16 mm and 13 mm respective diameters were used. Separators (GF/A glass fiber, GE Healthcare) were 18 mm diameter. Electrodes and separators were prepared in ambient atmosphere as well as handling of all coin cell components.

Two electrolyte stock solutions were prepared manually. Lithium perchlorate ($LiClO_4$) (99.99%, battery grade) and DMSO (anhydrous, ≥99.9%) were obtained from Sigma Aldrich. Milli-Q water was obtained from SPEX CertiPrep (Assurance® grade, Type I water). Batches of 2 mol kg^{-1} (molality, m) $LiClO_4$ in DMSO and 2 m $LiClO_4$ in water electrolyte stock solutions were prepared prior to coin cell assembly. 2 m $LiClO_4$ in DMSO stock

† https://github.com/jyik/ODACell

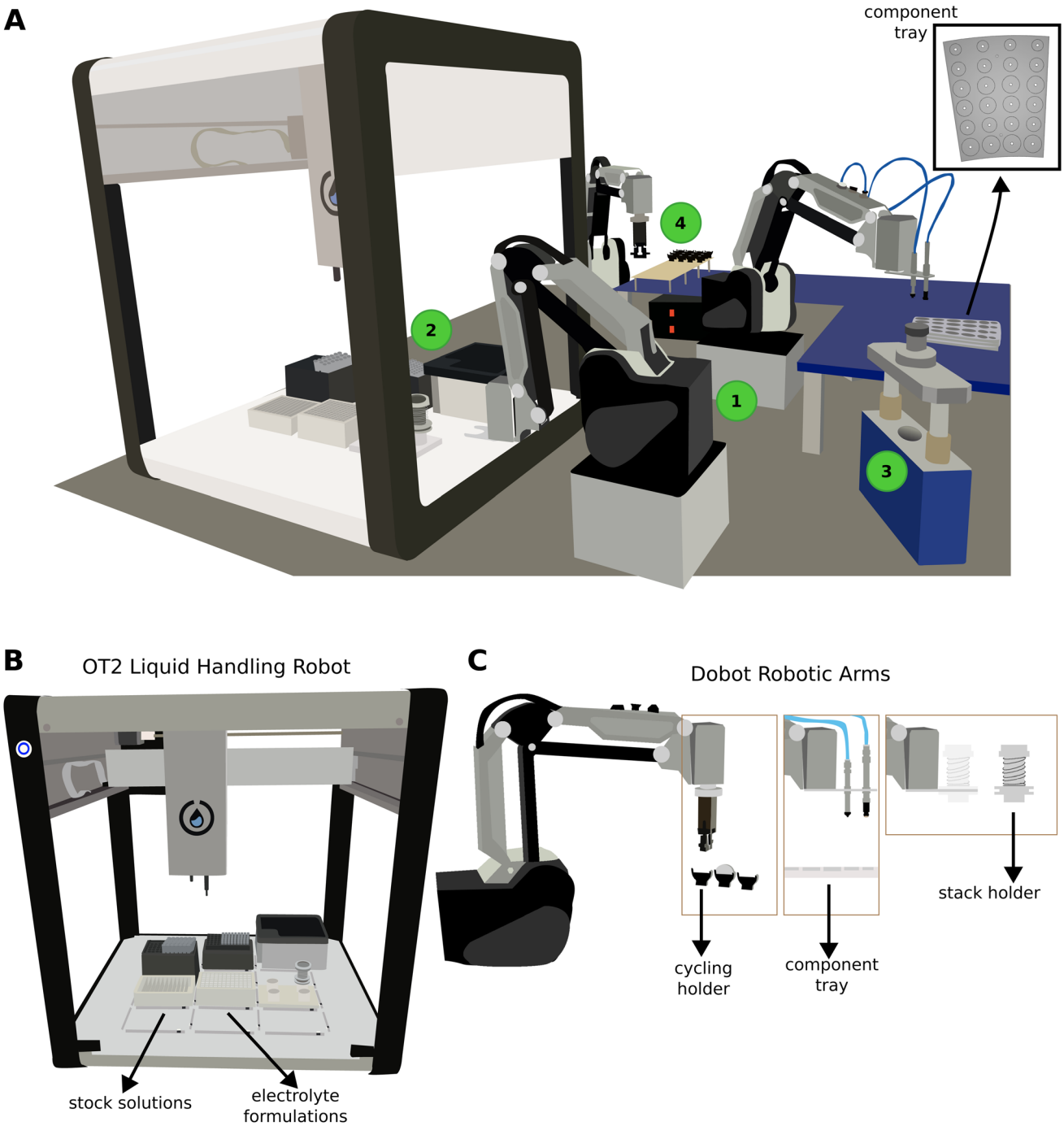

Fig. 1 Schematic illustration of the automated robotic assembly setup. (A) The four robots (three 4-axis robotic arms and one liquid handling robot) are detailed along with the elevated platform where the battery cycling station and coin cell components are placed. Numbered circles are placed at key positions in the assembly process: (1) placing coin cell components, (2) acquiring electrolyte, (3) crimping, and (4) cycling the coin cell. (B) The liquid handling robot where electrolyte formulation occurs. Stock solutions are loaded into the reservoirs and the robot can mix them together in the adjacent wells to formulate different electrolyte compositions. (C) The three 4-axis robotic arms handling the coin cell assembly and battery cycling. Each one has its own unique attachments to perform specific tasks.

solutions were stored under inert atmosphere and transferred into ambient atmosphere just before assembling a batch of coin cells. 2 m $LiClO_4$ in water stock solutions were prepared by mixing $LiClO_4$ salt with water just before assembling a batch of coin cells.

Experimentation

To evaluate the cell-to-cell variability and assembly reproducibility, 83 cells were assembled in six batches (three cells in the first batch, 16 cells per batch thereafter) using 2 m $LiClO_4$ in DMSO electrolyte.

To systematically explore the influence of water in the electrolyte, galvanostatic cycling performance of LFP||LTO full cells with electrolytes containing mixtures of water in DMSO were compared. The liquid handling robot prepared the first hybrid electrolyte by mixing 840 μL of 2 m $LiClO_4$ in DMSO and 160 μL of 2 m $LiClO_4$ in water. Mixing was done by aspirating and dispensing 700 μL of the mixture 20 times. The next hybrid electrolyte composed of 500 μL from the previous mixture and 500 μL from the 2 m $LiClO_4$ in DMSO stock solution using the same mixing procedure. The same operations for the third and fourth hybrid electrolytes were done, producing 16 vol%, 8 vol%, 4 vol%, and 2 vol% H_2O-electrolytes. 12 coin cells were assembled and cycled for each hybrid electrolyte. One electrolyte formulation was mixed, then a batch of coin cells were assembled; this process was repeated for the four hybrid electrolytes.

Considering the hygroscopicity of DMSO, the water content of the dried DMSO was measured after exposing it to laboratory environment for nine hours. Laboratory temperature and relative humidity were also recorded. Water content was quantified by Karl Fischer titration using Metrohm 851 Titrando (Switzerland).

Cycling procedure

Galvanostatic cycling was performed using a battery cycler with 16 total channels from Astrol Electronic AG, Switzerland. Since the cathode was oversized, recorded capacity was normalized with respect to the LTO active mass. The mean LTO active mass (8.84 mg) was used for all cells. The cycling procedure had a rest period of 2 hours for wetting. Charging and discharging cycles followed for 10 cycles using a constant C/2 rate (1C = 150 mA g^{-1}) translating to a constant current (CC) of 0.663 mA. The charging and discharging CC step was between the voltage range of 1.6 to 2.2 V.

Results and discussion

ODACell setup

The coin cell assembly process was as follows: a robotic arm equipped with a vacuum head loaded the positive casing, followed by the cathode, then separator onto a holder attached to another robotic arm (location 1 in Fig. 1A); the holder was then moved into the liquid handling robot and 45 μL of the desired electrolyte was dispensed (location 2 in Fig. 1A); the holder then returned to the previous position to receive the anode, spacer and spring, and the negative casing with gasket, sequentially (location 1 in Fig. 1A); upon placement of the negative casing, the robotic arm with the vacuum head applied a downward force on the stack to ensure flush closure of the cell; the holder with all the components entered the crimper to seal the coin cell (location 3 in Fig. 1A); the crimped coin cell was delivered to the cycling station by the robotic arm with the vacuum head, where another robotic arm with a gripper loaded the cell into an empty holder for galvanostatic cycling (location 4 in Fig. 1A).

The level of automation for ODACell extends from electrolyte formulation to electrochemical cycling and data collection. The only manual operations required of the user are to place and load the component trays (depicted in Fig. 1A) and load the electrolyte stock solutions. The user can load up to ten trays (40 cells) at a time. The electrolyte stock solutions are prepared manually in batches and then manually dispensed into designated wells. Once those two manual tasks are completed, the automated coin cell assembly and cycling can start. If a stock solution already matches the desired electrolyte formulation (such as the case for the reproducibility experiment), no mixing is done and the stock solution is used. Combinations of different electrolytes are mixed from the stock solutions (such as the case for the water series experiment) by the liquid handling robot. ODACell has automated the electrolyte formulation, coin cell assembly (including dispensing electrolyte), electrochemical cycling, data collection, and removal of finished or failed coin cells.

Based on the current cycling protocol, one cell takes *ca.* 42 hours to collect a data sample, of which 4 minutes is from assembling the cell as described in the previous paragraphs. Therefore, the current bottleneck is the battery cell cycling step. Currently, with 16 cycling channels, the setup is not capable of continuous assembly. Consequently, the number of channels in the setup will determine the bottleneck. We will soon increase the number of channels to 200 and then a 13 hour cycling protocol would enable continuous assembly and testing (where automated electrolyte formulation is done independently of assembly, achieved by parallelizing the orchestration). Depending on the desired battery evaluation procedure, a 13 hour cycling protocol is feasible. The choice of 10 cycles for this work was to be able to observe and compare the performance trends of the cells containing different hybrid electrolytes in the water concentration series experiments; and the choice of 2 hours rest period for wetting and C/2 cycling rate were not optimized in this work. Increasing the number of channels and decreasing the cycling time will reduce bottlenecks in the system to achieve higher throughput.

In the case of systems-level applications, such as assembling and cycling battery cells, the throughput is intrinsically lower compared to material-level applications. Stein *et al.*[22] provided a conceptual summary visualizing different throughputs of acceleration setups on a materials-interfaces-systems scale. While setups developed for characterization of materials and interfaces can acquire data within seconds,[5,16,22,23] testing an assembled cell may take months. The definition of high-throughput, therefore, can change depending on the application. For systems-level setups, a different approach on throughput can be considered that focuses on the initial experiment and continuous experimentation separately. If the assembling time for a batch and the testing time for each cell is the same as described earlier, then the throughput for data acquisition is limited by the assembly time. That is to say, for assembling and testing cells, the first cell will take the longest time to acquire data, but the subsequent cells will take much shorter time, assuming finished cells are continuously replaced with new cells. Failed cells and other complications may arise in the assembly or testing processes, but the average throughput should be consistent. ODACell is a step towards high-

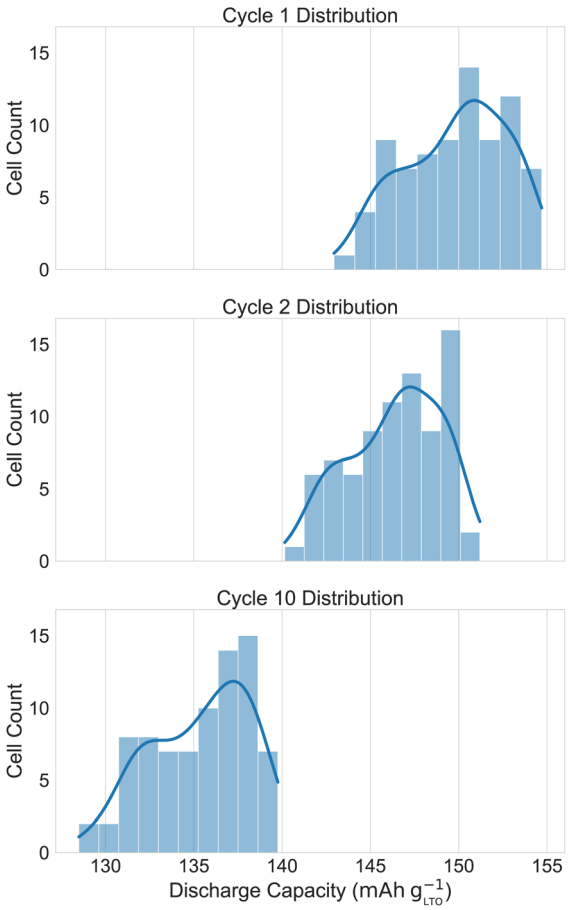

Fig. 2 Distribution of the discharge capacities for the 80 coin cells assembled by the automated robotic setup for cycle 1, 2, and 10. The mean and standard error for cycles 1, 2, and 10 are 149.8 ± 0.3 mA h g^{-1}, 146.4 ± 0.3 mA h g^{-1}, and 135.3 ± 0.3 mA h g^{-1}, respectively.

throughput and as such intended to demonstrate how the setup can be used for intelligent exploratory screening with high repeatability and analytical capabilities to detect novel candidate electrolyte systems.

Comparison of the presented setup to other setups developed by other groups is limited owing to the lack of publicly published setups. Commercially available robotic setups, such as the ones optimized for battery applications,[24,25] on the other hand, are not easily modified or integrated with other machines, making it hard to adjust and customize any of the hardware and software. With publicly publishable setups, such as ODACell, a modular, flexible system can be made, where any addition of robots or changes in software can be implemented and orchestrated together. Alternatively, setups, such as Clio,[5] can control static machinery, such as pumps and valves, to move samples without the flexibility of a robotic arm. Comparing ODACell to AutoBASS,[6] another systems-level automated setup, ODACell has the ability to formulate electrolytes in additional to coin cell assembly and electrolyte dispensing which AutoBASS is limited to. AutoBASS can, in principle, dispense different electrolytes, but the mixing capabilities to achieve a homogeneous solution is limited compared to ODACell. AutoBASS has a camera to monitor the component placement, which will be included in ODACell in the future. AutoBASS has one less robotic arm than ODACell making it more space efficient but also removing any potential flexibility an additional robotic arm would provide. ODACell's unique approach and combination set of tools allow automation to span more of the battery material research workflow (*e.g.* electrolyte discovery process) in a single system. Another robotic setup, Poseidon, has been developed that is capable of electrolyte formulation, Raman spectroscopic characterization, and cycling evaluation.[8] Although Poseidon has capabilities that extend beyond ODACell, it lacks batch cell assembly and evaluation owing to only having a single robotic arm; therefore, Poseidon may not be suitable for high-throughput combinatorial experimentation.

Reproducibility

Fig. 2 shows the distribution of the cycle 1, 2, and 10 discharge capacities. Fig. 3 shows the charge and discharge curves for cycle 10. The mean and standard error for cycles 1, 2, and 10 are 149.8 ± 0.3 mA h g^{-1}, 146.4 ± 0.3 mA h g^{-1}, and 135.1 ± 0.3 mA h g^{-1}, respectively. For cycle 10, the standard error translates to 3.0 mA h g^{-1} or 2.1% standard deviation for sampled data around the mean. The distribution is negatively skewed (Fisher–Pearson coefficient of skewness = − 0.34 for cycle 1) and lacks an overt shape. In contrast, Gaussian distributions are seen in the discharge capacities of the cells from the AutoBASS robotic assembly setup.[6] However, the different cell chemistries may partially explain the discrepancy. In non-aqueous systems, the assembly process must be done under inert atmosphere because of the reactivity of the electrolyte with moisture. In contrast, the selected chemistry of our system is more tolerant to air and moisture, but still experience side reactions, as the coulombic efficiency is less than 100%. The longer the electrolyte is exposed to the environment, the higher the risk that O_2 and H_2O adversely influence cell performance.[26] Future updates to ODACell will include an automated vial de-/capping accessory. Important to note, no electrode passivation layers (*e.g.* solid electrolyte interphase) are known to form in our system.[27]

The exposure of the electrolyte to air before assembly could be an influential factor affecting the performance distribution. As previously mentioned, the current setup has the electrolyte open during assembly. The electrolyte is hygroscopic so water is gradually absorbed into the electrolyte; however, exposure to air was limited by storing the electrolyte under inert atmosphere until use and making fresh electrolyte stock solution for each batch. Fig. 4 shows the amount of water in DMSO after exposing it to the ambient atmosphere over time. Although the temperature of the room was controlled, the relative humidity was not; the highest humidity was recorded approximately at noon of a working day, four hours after exposure. Humidity affects the rate of absorption,[28] but even after nine hours, the accumulated water content in the DMSO is still less than 1% by weight. The addition of $LiClO_4$ to DMSO will raise the hygroscopicity of the mixture in comparison to DMSO alone, thus the accumulated water contents for the electrolytes are greater than concluded

with the DMSO calibration curve. We limited the time of exposure to a single working day because the exposure of electrolyte to the ambient atmosphere ranged from 5 minutes for the first cell assembled in a batch to 45 minutes for the last cell in a batch. The accuracy of the electrolyte dispensing is approximately 1% based on manufacturer specifications, which also minutely contribute to the performance distribution. To reduce any performance deviations due to contamination of electrode material on the suction cups, two vacuum heads were deployed; one vacuum head picked up the cathode casing, cathode and separator, while the other vacuum head picked up the anode, spacer and spring, and anode casing. Additionally, a chemically inert (polyether ether ketone, PEEK) vacuum head insert was attached to the suction cup coming in direct contact with the porous cathode material surface.

Misalignment of components and electrical contact issues were additional sources of error. Although the robotic arm's vacuum head drop placement was centered in the holder, the cathode or separator could still slightly deviate from center position due to the separator being dropped onto the curved cathode surface. Dropping the spacer and spring on the stack could also shift the weight of the stack causing misalignment. Small variations in the electrodes' mass loading will also influence the performance distribution but its effect was minimized by using commercial electrodes (active material mass standard deviation *ca.* 5%) instead of inhouse-made electrodes (active material mass standard deviation *ca.* 20%). Commercial electrodes are manufactured to have reliable specified capacity whereas inhouse-made electrodes could have wide variations depending on the slurry coating process.

In Fig. 3, areas with similarly performing cells overlap and have higher saturation of color. The standard error throughout the cycles remained 0.3 mA h g^{-1}, and the higher sample size translates to a smaller standard error. However, in practice, 80 replicates are infeasible and a more realistic goal is 12 replicates, which is demonstrated with the water concentration series.

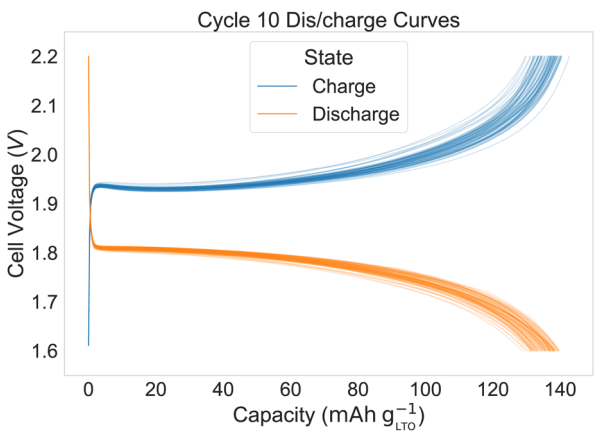

Fig. 3 Charge and discharge curves for cycle 10 of the 80 $LiFePO_4||Li_4Ti_5O_{12}$ full cells with dimethyl sulfoxide electrolyte at C/2 rate (1C = 150 mA g^{-1}). The denser the lines, the bolder the color.

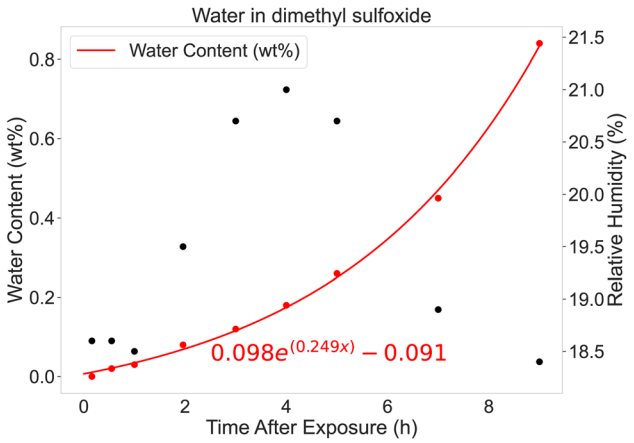

Fig. 4 Amount of water absorbed into dimethyl sulfoxide (DMSO) after exposing it to ambient laboratory atmosphere at the liquid handling robot. Temperature of the room was controlled at 19.7 ± 0.1 °C. Coefficient of determination for the exponential fit $R^2 = 0.9985$.

Water concentration series

A further motivation for the water concentration series experiments, besides systematically exploring the influence of water in the electrolyte due to air exposure, is to demonstrate the entire automated workflow for electrolyte discovery, from electrolyte formulation to performance testing, in a practical application. Fig. 5 shows the galvanostatic cycling data for cells with electrolytes containing variable amounts of added water. The cells used to determine reproducibility are used for the 0 vol% H_2O-electrolyte group. In Fig. 5A and B, the mean capacities decrease with increasing water content. The trend is consistent throughout the 10 cycles. The performance between 4 vol%, 2 vol%, and 0% H_2O-electrolyte groups are, however, indistinguishable from each other; the mean discharge capacities for cycle 10 were 120.6 ± 5.7 mA h g^{-1}, 133.0 ± 0.7 mA h g^{-1}, 135.3 ± 0.6 mA h g^{-1}, 135.3 ± 0.6 mA h g^{-1}, and 135.3 ± 0.3 mA h g^{-1} for the 16 vol%, 8 vol%, 4 vol%, 2 vol%, and 0% H_2O-electrolyte groups, respectively.

The coulombic efficiency for the different water content electrolytes in Fig. 5C show that the 16 vol% H_2O-electrolyte group is consistently lower compared to the other three dilution groups throughout the 10 cycles. The 8 vol%, 4 vol%, 2 vol%, and 0% H_2O-electrolyte cells have similar coulombic efficiencies (99.0 ± 0.2%, 99.4 ± 0.1%, 98.9 ± 0.2%, 99.3 ± 0.1% respectively for cycle 10). Side reactions involving water are driving the capacity and efficiency trends.

Performance trends between the different hybrid electrolytes are largely due to the water content in the system. Increasing the amount of water increases the prevalence of water reduction due to the narrow stability window of water (1.23 V). DMSO, however, can suppress interfacial electrochemical reactions of water molecules by entering the cation solvation sheath directly and form DMSO–H_2O H-bond networks that effectively reduce the activity of water molecules.[29] The H-bond structure in the

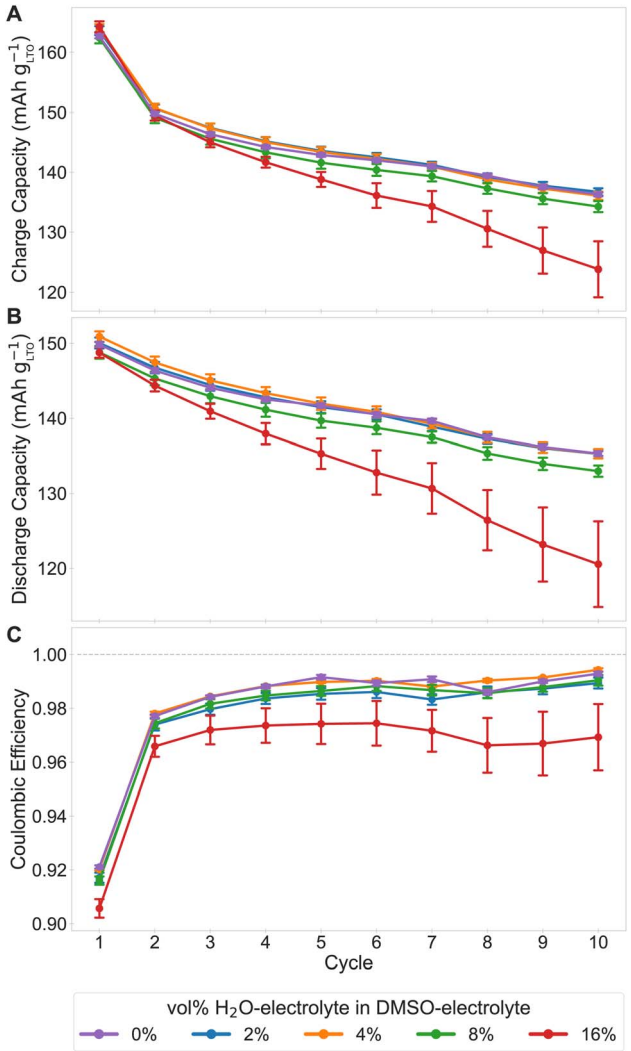

Fig. 5 Specific capacity and energy trends with different volume percent of H_2O-electrolyte in dimethyl sulfoxide (DMSO)-electrolyte. Error bars are standard error. (A and B) Charge and discharge specific capacity normalized to the mean anode active material (lithium titanate, LTO) *vs.* cycle, (C) coulombic efficiency computed from (A) and (B) *vs.* cycle.

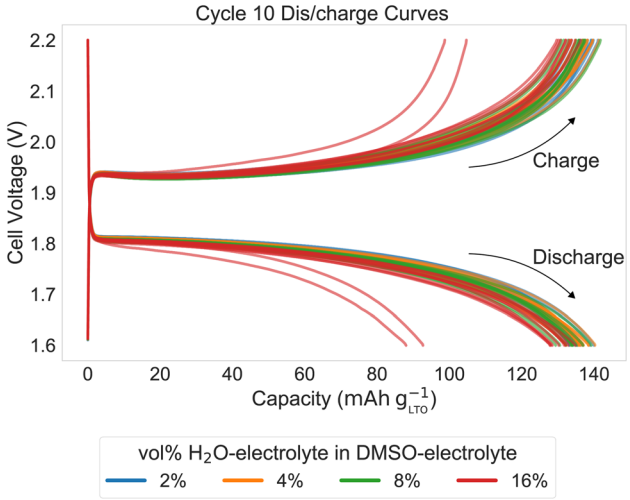

Fig. 6 Charge and discharge curves of the assembled coin cells ($LiFePO_4$||$Li_4Ti_5O_{12}$ full cells) with varying water content in the dimethyl sulfoxide-electrolyte for cycle 10. Two possible outliers are seen.

solution affects the water reduction reaction so small amounts of water in the DMSO hybrid electrolyte is tolerable and water reduction can be largely suppressed. With increased amounts of water, the DMSO–H_2O H-bond network is less prevalent, becoming unable to effectively suppress the water reduction reaction. Consequently, small amounts of gas from water reduction can cause increased internal impedance from mechanical disintegration of the electrodes or other side reactions due to local pH changes at the electrodes.[26] Water reduction likely explains the lower coulombic efficiencies and capacities evident from the trends of Fig. 5. Nevertheless, the 2 vol% and 4 vol% H_2O-electrolyte cells have similar capacities after 10 cycles as these concentrations of water are insufficient to significantly affect cell performance. The relationship between capacity drop and water content is not trivial. However, differences between the hybrid electrolytes and any possible outliers would become more evident with more cycles.

The charge/discharge curves of Fig. 6 reveal two possible outliers. These two cells both belong to the 16 vol% H_2O-electrolyte group and exhibited faster capacity fade compared to the other cells in the group. These two cells contribute to the increased variance for the group (visualized by larger error bars in Fig. 5). If the two outliers were removed from the analysis, the relative standard deviation would decrease from 15.7% (standard error 5.7 mA h g^{-1}) to 2.4% (standard error 1.0 mA h g^{-1}). The increasing standard deviation with increasing water content could be also be attributed to the electrolyte mixing process. If the two stock solutions were not sufficiently mixed, the resulting electrolyte solution would not be homogenous and, subsequently, cells could receive electrolyte containing varying water content. This is a potential limitation since there might be electrolyte mixtures that cannot be properly mixed with the setup's current capabilities.

Overall, the water concentration series demonstrates that the DMSO-based electrolyte can tolerate up to 4% of water in its formulation without observable performance degradation within 10 cycles and reinforces the necessity of replicates in practice. Presence of side reactions can cause wider variation in the data; therefore, more complex systems may require more replicates to have observable effects on performance. The relative standard deviation was 1.4%, 1.6%, 1.9%, and 15.7% for 2, 4, 8, and 16 vol% H_2O-electrolyte cells, respectively. Since the variance of the discharge capacity with little water content (2, 4, and 8 vol% in the water concentration series) in the electrolyte is similar to the electrolyte without any added water, 12 replicates to evaluate reproducibility, instead of 80 replicates, would have sufficed. It should also be noted again that the standard deviation scales with increasing complexity of the electrolyte formulation and the increasing potential interactions between all components within the electrolyte, thereof. Although the

current robotic setup may suffer from the open system of the electrolyte formulation step and limitations in the mixing procedure, it is a methodology that can handle future high-throughput tests and closed-loop exploration of the electrolyte design space. There already exists frameworks for combining automation and machine learning to achieve autonomous setups in different applications.[30,31]

In future work, we will adapt a framework and incorporate an optimization algorithm, such as a Bayesian optimizer, *e.g.* to evaluate the influence of oxygen scavengers and other electrolyte additives in aqueous lithium-ion batteries.[32] In addition to building upon the current setup, improvements to this setup could further increase reproducibility and reduce variance between the performance of cells. We have planned to introduce a camera system as well as position calibration for the setup, ensuring proper placement of assembly components. Furthermore, as previously discussed, we plan on designing an apparatus to store electrolytes in a closed system to reduce extended periods of exposure to ambient atmosphere.

Conclusions

In this work, the capabilities of ODACell, an automated robotic coin cell assembly and electrolyte formulation setup was demonstrated. A conservative estimate of the assembly failure rate for the current setup is 5% from the 131 coin cells assembled for this work. Component misalignment causing short-circuits and electrical contact issues were the main sources of failure. The relative standard deviation of cycle 10's discharge capacity was 2% for our system. The proposed improvements would decrease the variability of the cells assembled making the setup reliable and affordable for research of electrolytes compatible with the ambient laboratory atmosphere.

We demonstrated the seamless integration of a liquid handling robot into the assembly setup and tested different water contents in the electrolyte. Our unique approach and combination of tools distinguishes our setup from others. With the electrolyte formulations made by the liquid handling robot, consistent and reproducible performance metrics between the formulations were observed. Noticeably, there was little difference in capacity and coulombic efficiency between 4 vol%, 2 vol%, and 0% H_2O-electrolyte cells, suggesting a nontrivial relationship of electrolytes containing mixtures of small amounts of water in DMSO and cycling performance. The water concentration series experiment demonstrates the tolerance of DMSO-based electrolytes to minor amounts (up to 4%) of water in its formulation without significant detriment to the performance of batteries. This is necessary if Li-ion batteries are to be assembled under ambient conditions. Dry rooms are expensive in terms of cost and energy. Moreover, this reinforces the need for more replicates when exploring different liquid electrolyte compositions in order to accurately determine trends and optimize liquid electrolyte design. The electrolyte evaluated herein may form a basis for further exploration of water-tolerable electrolyte for higher voltage Li-ion batteries.

Data availability

All the code and data associated with this work can be found at **https://github.com/jyik/ODACell** with **https://doi.org/10.5281/zenodo.7598082**. The analysis scripts as well as data files are compressed into .zip files alongside the python files for the robot orchestration.

Author contributions

Jackie T. Yik: investigation, software, formal analysis, writing – original draft, writing – review & editing, visualization. Leiting Zhang: methodology, conceptualization, resources, writing – review & editing, supervision. Jens Sjölund: resources, writing – review & editing, supervision. Xu Hou: resources, writing – review & editing. Per H. Svensson: writing – review & editing. Kristina Edström: conceptualization, project administration, funding acquisition. Erik J. Berg: methodology, conceptualization, resources, writing – review & editing, supervision, funding acquisition, project administration.

Conflicts of interest

There are no conflicts to declare.

Acknowledgements

This research was financially supported by the Swedish Energy Agency (Grant 50119-1), Stiftelsen för Strategisk Forskning (SSF, FFL18-0269), Knut and Alice Wallenberg (KAW) Foundation (Grant 2017.0204) and StandUp for Energy for base funding. This research was also supported by Wallenberg AI, Autonomous Systems and Software Program (WASP) funded by the KAW Foundation.

References

1 J. Amici, P. Asinari, E. Ayerbe, P. Barboux, P. Bayle-Guillemaud, R. J. Behm, M. Berecibar, E. Berg, A. Bhowmik, S. Bodoardo, I. E. Castelli, I. Cekic-Laskovic, R. Christensen, S. Clark, R. Diehm, R. Dominko, M. Fichtner, A. A. Franco, A. Grimaud, N. Guillet, M. Hahlin, S. Hartmann, V. Heiries, K. Hermansson, A. Heuer, S. Jana, L. Jabbour, J. Kallo, A. Latz, H. Lorrmann, O. M. Løvvik, S. Lyonnard, M. Meeus, E. Paillard, S. Perraud, T. Placke, C. Punckt, O. Raccurt, J. Ruhland, E. Sheridan, H. Stein, J.-M. Tarascon, V. Trapp, T. Vegge, M. Weil, W. Wenzel, M. Winter, A. Wolf and K. Edström, A Roadmap for Transforming Research to Invent the Batteries of the Future Designed within the European Large Scale Research Initiative BATTERY 2030+, *Adv. Energy Mater.*, 2022, **12**, 2102785.

2 H. S. Stein and J. M. Gregoire, Progress and prospects for accelerating materials science with automated and autonomous workflows, *Chem. Sci.*, 2019, **10**, 9640–9649.

3 P. Liu, B. Guo, T. An, H. Fang, G. Zhu, C. Jiang and X. Jiang, High throughput materials research and development for lithium ion batteries, *J. Materiomics*, 2017, **3**, 202–208.
4 A. Dave, J. Mitchell, K. Kandasamy, H. Wang, S. Burke, B. Paria, B. Póczos, J. Whitacre and V. Viswanathan, Autonomous Discovery of Battery Electrolytes with Robotic Experimentation and Machine Learning, *Cell Rep. Phys. Sci.*, 2020, **1**, 100264.
5 A. Dave, J. Mitchell, S. Burke, H. Lin, J. Whitacre and V. Viswanathan, Autonomous optimization of non-aqueous Li-ion battery electrolytes *via* robotic experimentation and machine learning coupling, *Nat. Commun.*, 2022, **13**, 5454.
6 B. Zhang, L. Merker, A. Sanin and H. S. Stein, Robotic cell assembly to accelerate battery research, *Digital Discovery*, 2022, **1**, 755–762.
7 S. Matsuda, K. Nishioka and S. Nakanishi, High-throughput combinatorial screening of multi-component electrolyte additives to improve the performance of Li metal secondary batteries, *Sci. Rep.*, 2019, **9**, 6211.
8 P. H. Svensson, P. Yushmanov, A. Tot, L. Kloo, E. Berg and K. Edström, Robotised screening and characterisation for accelerated discovery of novel Lithium-ion battery electrolytes: Building a platform and proof of principle studies, *Chem. Eng. J.*, 2023, **455**, 140955.
9 J. E. Harlow, X. Ma, J. Li, E. Logan, Y. Liu, N. Zhang, L. Ma, S. L. Glazier, M. M. E. Cormier, M. Genovese, S. Buteau, A. Cameron, J. E. Stark and J. R. Dahn, A Wide Range of Testing Results on an Excellent Lithium-Ion Cell Chemistry to be used as Benchmarks for New Battery Technologies, *J. Electrochem. Soc.*, 2019, **166**, A3031–A3044.
10 P. Dechent, S. Greenbank, F. Hildenbrand, S. Jbabdi, D. U. Sauer and D. A. Howey, Estimation of Li-Ion Degradation Test Sample Sizes Required to Understand Cell-to-Cell Variability, *Batteries Supercaps*, 2021, **4**, 1821–1829.
11 P. M. Attia, A. Grover, N. Jin, K. A. Severson, T. M. Markov, Y.-H. Liao, M. H. Chen, B. Cheong, N. Perkins, Z. Yang, P. K. Herring, M. Aykol, S. J. Harris, R. D. Braatz, S. Ermon and W. C. Chueh, Closed-loop optimization of fast-charging protocols for batteries with machine learning, *Nature*, 2020, **578**, 397–402.
12 M. Fichtner, K. Edström, E. Ayerbe, M. Berecibar, A. Bhowmik, I. E. Castelli, S. Clark, R. Dominko, M. Erakca, A. A. Franco, A. Grimaud, B. Horstmann, A. Latz, H. Lorrmann, M. Meeus, R. Narayan, F. Pammer, J. Ruhland, H. Stein, T. Vegge and M. Weil, Rechargeable Batteries of the Future—The State of the Art from a BATTERY 2030+ Perspective, *Adv. Energy Mater.*, 2022, **12**, 2102904.
13 A. Benayad, D. Diddens, A. Heuer, A. N. Krishnamoorthy, M. Maiti, F. L. Cras, M. Legallais, F. Rahmanian, Y. Shin, H. Stein, M. Winter, C. Wölke, P. Yan and I. Cekic-Laskovic, High-Throughput Experimentation and Computational Freeway Lanes for Accelerated Battery Electrolyte and Interface Development Research, *Adv. Energy Mater.*, 2022, **12**, 2102678.
14 T. Lombardo, M. Duquesnoy, H. El-Bouysidy, F. Årén, A. Gallo-Bueno, P. B. Jørgensen, A. Bhowmik, A. Demortière, E. Ayerbe, F. Alcaide, M. Reynaud, J. Carrasco, A. Grimaud, C. Zhang, T. Vegge, P. Johansson and A. A. Franco, Artificial Intelligence Applied to Battery Research: Hype or Reality?, *Chem. Rev.*, 2022, **122**, 10899–10969.
15 A. Ludwig, Discovery of new materials using combinatorial synthesis and high-throughput characterization of thin-film materials libraries combined with computational methods, *npj Comput. Mater.*, 2019, **5**, 70.
16 L. Yang, J. A. Haber, Z. Armstrong, S. J. Yang, K. Kan, L. Zhou, M. H. Richter, C. Roat, N. Wagner, M. Coram, M. Berndl, P. Riley and J. M. Gregoire, Discovery of complex oxides *via* automated experiments and data science, *Proc. Natl. Acad. Sci. U. S. A.*, 2021, **118**, e2106042118.
17 E. McCalla, M. Parmaklis, S. Rehman, E. Anderson, S. Jia, A. Hebert, K. Potts, A. Jonderian, T. Adhikari and M. Adamič, Combinatorial methods in advanced battery materials design, *Can. J. Chem.*, 2022, **100**, 132–143.
18 Y. Wang, P. He and H. Zhou, Olivine $LiFePO_4$: development and future, *Energy Environ. Sci.*, 2011, **4**, 805–817.
19 C. P. Sandhya, B. John and C. Gouri, Lithium titanate as anode material for lithium-ion cells: a review, *Ionics*, 2014, **20**, 601–620.
20 M. Wang, X. Dong, I. C. Escobar and Y.-T. Cheng, Lithium Ion Battery Electrodes Made Using Dimethyl Sulfoxide (DMSO)—A Green Solvent, *ACS Sustainable Chem. Eng.*, 2020, **8**, 11046–11051.
21 D. Wu, W. Y. Zhang, H. J. Feng, Z. J. Zhang, X. Y. Chen and P. Cui, Mechanistic Insights into the Intermolecular Interaction and Li^+ Solvation Structure in Small-Molecule Crowding Electrolytes for High-Voltage Aqueous Supercapacitors, *ACS Appl. Energy Mater.*, 2022, **5**, 12067–12077.
22 H. S. Stein, A. Sanin, F. Rahmanian, B. Zhang, M. Vogler, J. K. Flowers, L. Fischer, S. Fuchs, N. Choudhary and L. Schroeder, From materials discovery to system optimization by integrating combinatorial electrochemistry and data science, *Curr. Opin. Electrochem.*, 2022, **35**, 101053.
23 A. Pomberger, N. Jose, D. Walz, J. Meissner, C. Holze, M. Kopczynski, P. Müller-Bischof and A. Lapkin, Automated pH Adjustment Driven by Robotic Workflows and Active Machine Learning, *Chem. Eng. J.*, 2023, **451**, 139099.
24 *Automation of Integrated R&D Workflows*, 2022, **https://www.chemspeed.com/integrated-solutions/**.
25 *The Cell Assembly & Sealing System*, 2022, **https://www.cellerate.co.uk/products**.
26 Y. Sui and X. Ji, Anticatalytic Strategies to Suppress Water Electrolysis in Aqueous Batteries, *Chem. Rev.*, 2021, **121**, 6654–6695.
27 K. Xu, Electrolytes and Interphases in Li-Ion Batteries and Beyond, *Chem. Rev.*, 2014, **114**, 11503–11618.

28 R. G. LeBel and D. A. I. Goring, Density, Viscosity, Refractive Index, and Hygroscopicity of Mixtures of Water and Dimethyl Sulfoxide, *J. Chem. Eng. Data*, 1962, **7**, 100–101.
29 Q. Nian, X. Zhang, Y. Feng, S. Liu, T. Sun, S. Zheng, X. Ren, Z. Tao, D. Zhang and J. Chen, Designing Electrolyte Structure to Suppress Hydrogen Evolution Reaction in Aqueous Batteries, *ACS Energy Lett.*, 2021, **6**, 2174–2180.
30 F. Häse, L. M. Roch and A. Aspuru-Guzik, Chimera: enabling hierarchy based multi-objective optimization for self-driving laboratories, *Chem. Sci.*, 2018, **9**, 7642–7655.
31 M. Seifrid, R. J. Hickman, A. Aguilar-Granda, C. Lavigne, J. Vestfrid, T. C. Wu, T. Gaudin, E. J. Hopkins and A. Aspuru-Guzik, Routescore: Punching the Ticket to More Efficient Materials Development, *ACS Cent. Sci.*, 2022, **8**, 122–131.
32 L. Zhang, X. Hou, K. Edström and E. J. Berg, Reactivity of TiS_2 Anode towards Electrolytes in Aqueous Lithium-Ion Batteries, *Batteries Supercaps*, 2022, **5**, e202200336.